Supporting Information

Direct Synthesis of Higher Alcohols from Syngas over Modified

Mo$_2$C Catalysts under Mild Reaction Conditions

Caiqi Wang[a,b], Hailing Yu[a,b], Tiejun Lin[a], Xingzhen Qi[a,b], Fei Yu[a], Liangshu Zhong[a,c,*],

Yuhan Sun[a,c,*]

[a] CAS Key Laboratory of Low-Carbon Conversion Science and Engineering, Shanghai

Advanced Research Institute, Chinese Academy of Sciences, Shanghai 201203, P.R.

China

[b] University of the Chinese Academy of Sciences, Beijing 100049, P.R. China

[c] School of Physical Science and Technology, ShanghaiTech University, Shanghai

201203, P.R. China

* Corresponding author.

E-mail: zhongls@sari.ac.cn (L. Zhong), sunyh@sari.ac.cn (Y. Sun).

Table S1 The element content of various catalysts determined by ICP-OES.

Samples	Content (wt%)		
	Rh	K	Mo
Mo_2C	-	-	74.5
Rh/Mo_2C	1.8	-	73.5
RhK/Mo_2C	1.6	4.8	70.3
K/Mo_2C	-	5.2	71.4

Table S2 The catalytic performances for syngas conversion over Rh/AC and RhK/AC catalysts.

Catalysts	CO Conversion %	CO_2 Selectivity	Selectivity (C%, free of CO_2)				
			CH_3OH	$C_{2+}Oxy$	Olefins	CH_4	$C_{2+}Alkane$
Rh/AC	1.3	11.8	10.5	20.2	5.0	45.0	19.3
RhK/AC	4.5	25.0	74.1	5.0	2.2	14.9	3.8

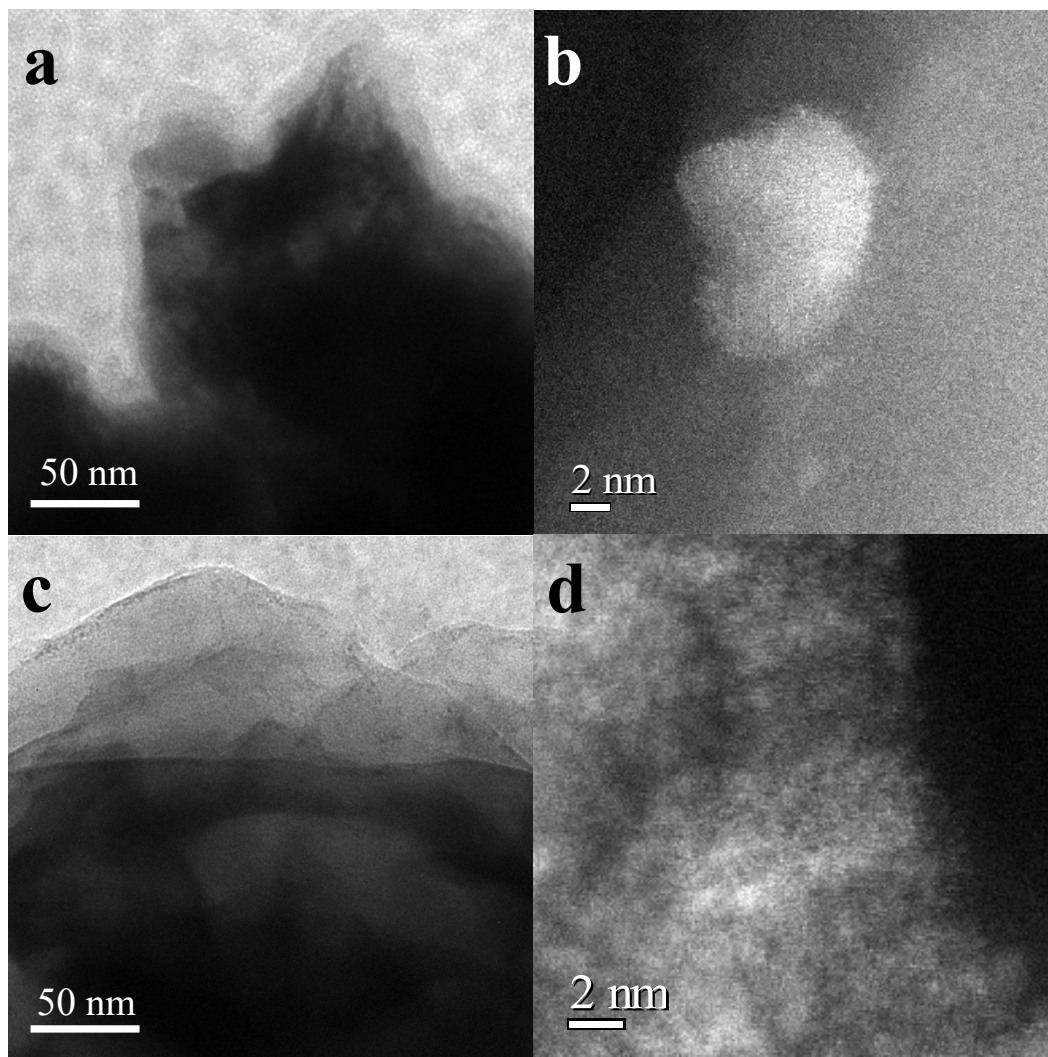Reaction conditions: 290 °C, $H_2/CO = 1$, 3 MPa, GHSV = 1200 mL·g^{-1}·h^{-1}.

Figure S1 TEM and HAADF-STEM images of the reduced catalysts. (a, b) Rh/Mo$_2$C, (c, d) RhK/Mo$_2$C.
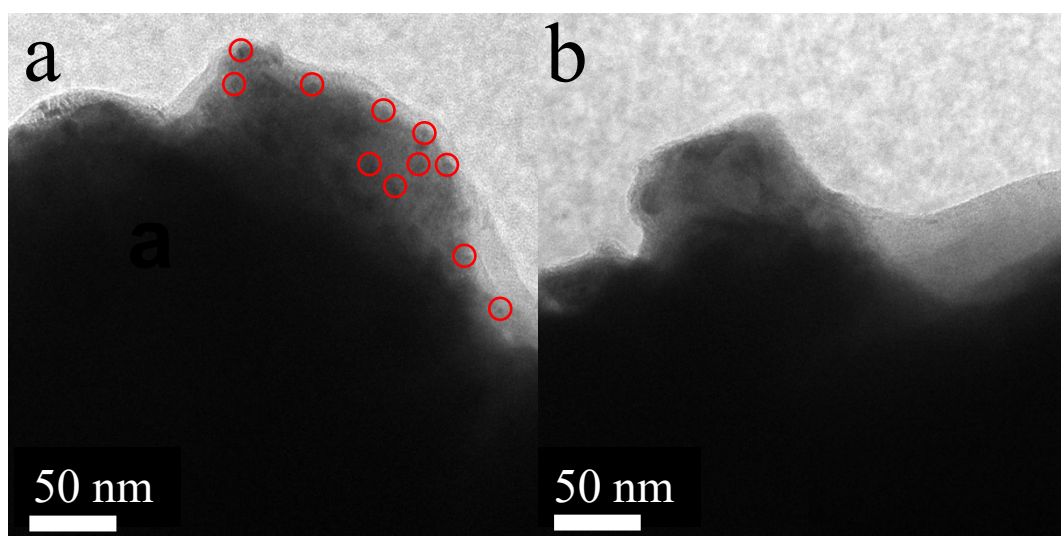
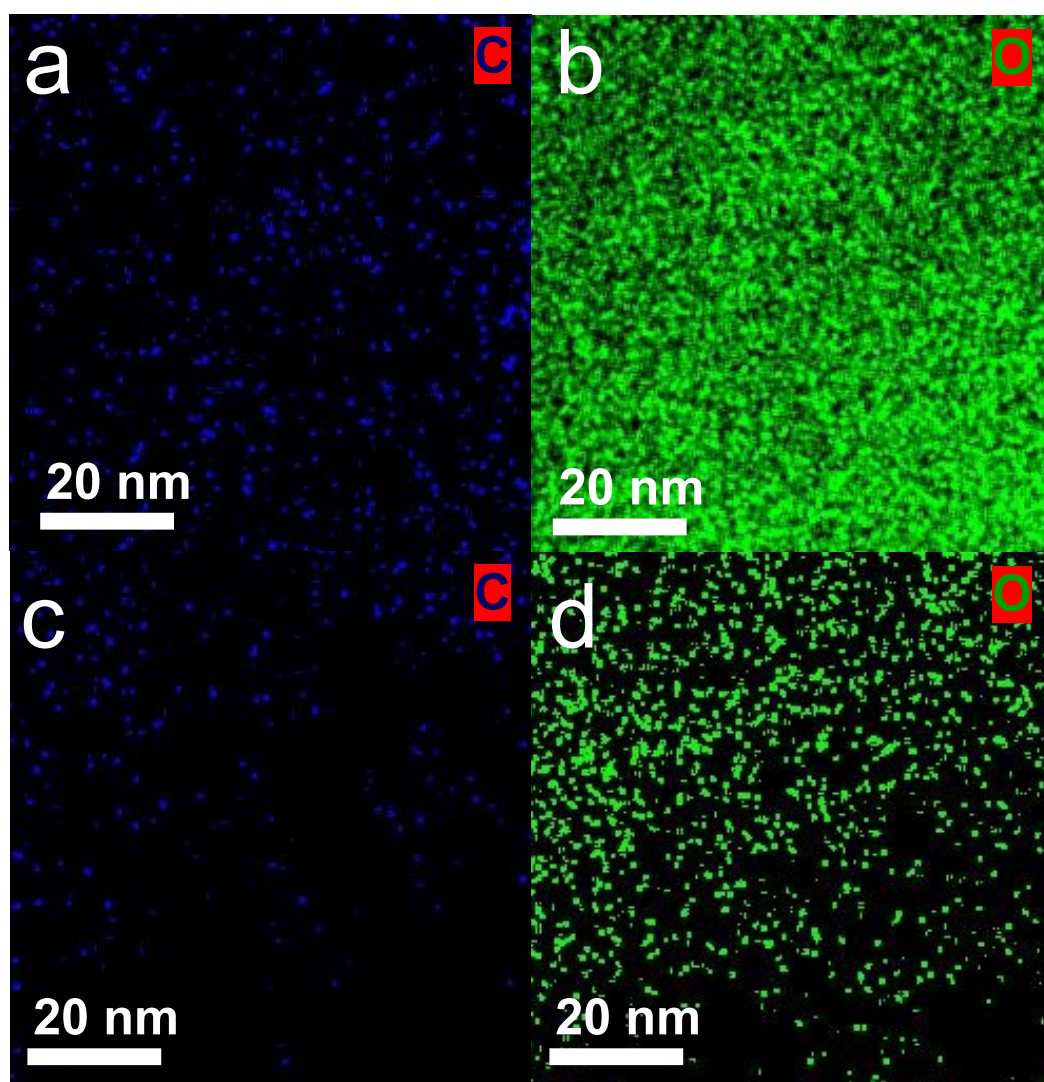Figure S2 TEM images of the spent catalysts. (a) Rh/Mo$_2$C, (b) RhK/Mo$_2$C.

Figure S3 Elemental mapping of C and O for spent Rh/Mo$_2$C (a, b) and
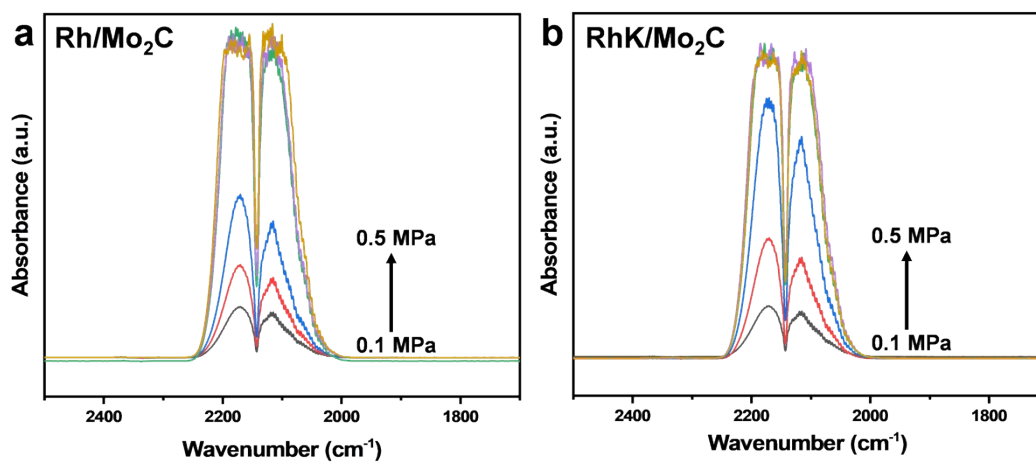
RhK/Mo$_2$C (c, d) catalysts.

Figure S4 In situ DRIFTs of CO adsorption from 0.1 to 0.5 MPa at 50 °C over Rh/Mo$_2$C (a) and RhK/Mo$_2$C (b) catalysts.
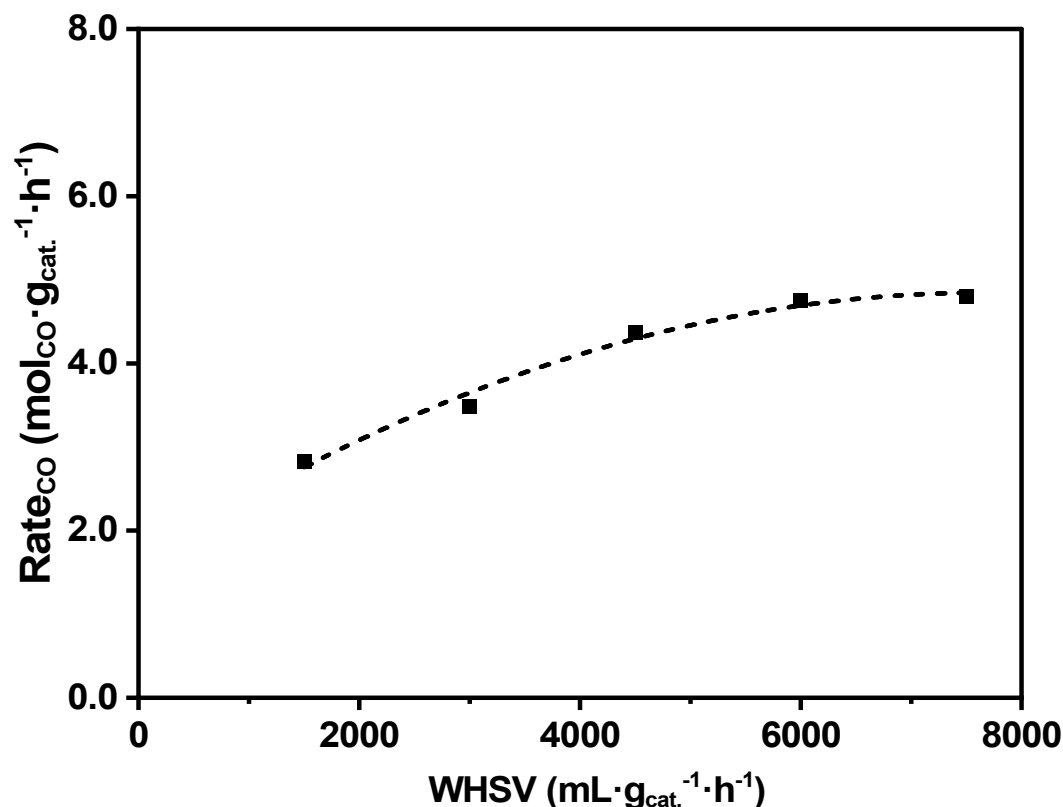
Figure S5 Dependence of CO consumption rate on WHSV.

(Conditions: H_2/CO=1, 290 °C, 1 MPa, 0.4 g of catalyst diluted with 2 g quartz)

For kinetic study, the diffusion effects were excluded by adjusting the WHSV over RhK/Mo_2C catalyst. With the increase of WHSV from 1500 to 7500 mL·$g_{cat.}^{-1}$·h^{-1} (Figure S5), CO consumption rate increased and then remained almost constant when WHSV reached 6000 mL·$g_{cat.}^{-1}$·h^{-1}, demonstrating a negligible effect on mass-transfer diffusion when WHSV was higher than 6000 mL·$g_{cat.}^{-1}$·h^{-1}. In the kinetic study, WHSV of 7500 mL·$g_{cat.}^{-1}$·h^{-1} was used to avoid the effect of mass transfer. In addition, to exclude the effect of heat transfer, 0.4 g of catalyst was diluted with 2 g quartz sand to remove the reaction heat.
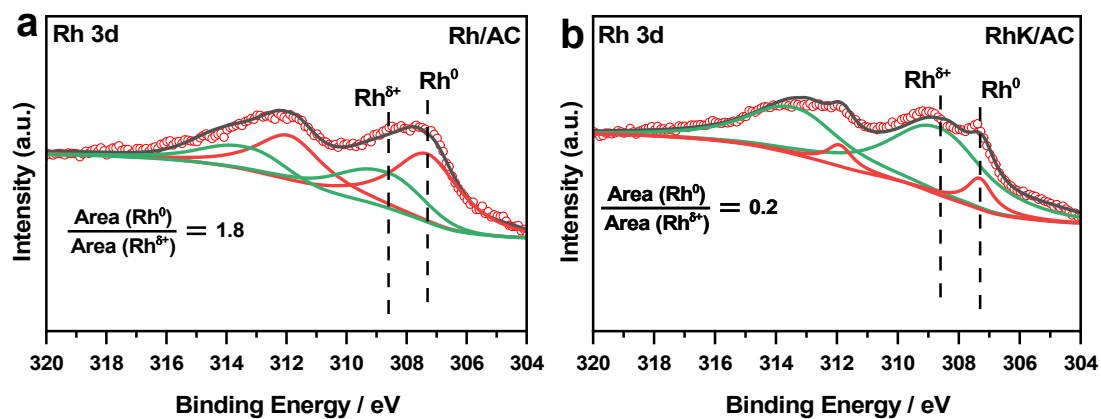
Figure S6 Rh 3d XPS spectra of (a) Rh/AC, (b) RhK/AC after reduction in syngas flow.
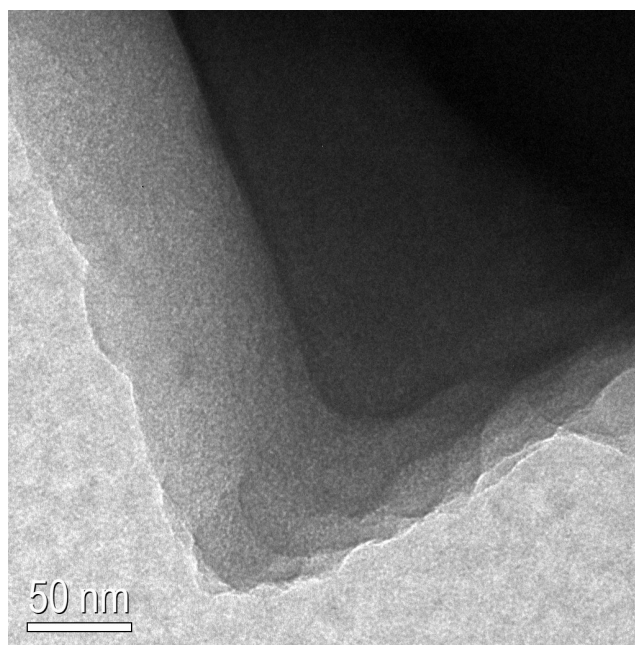

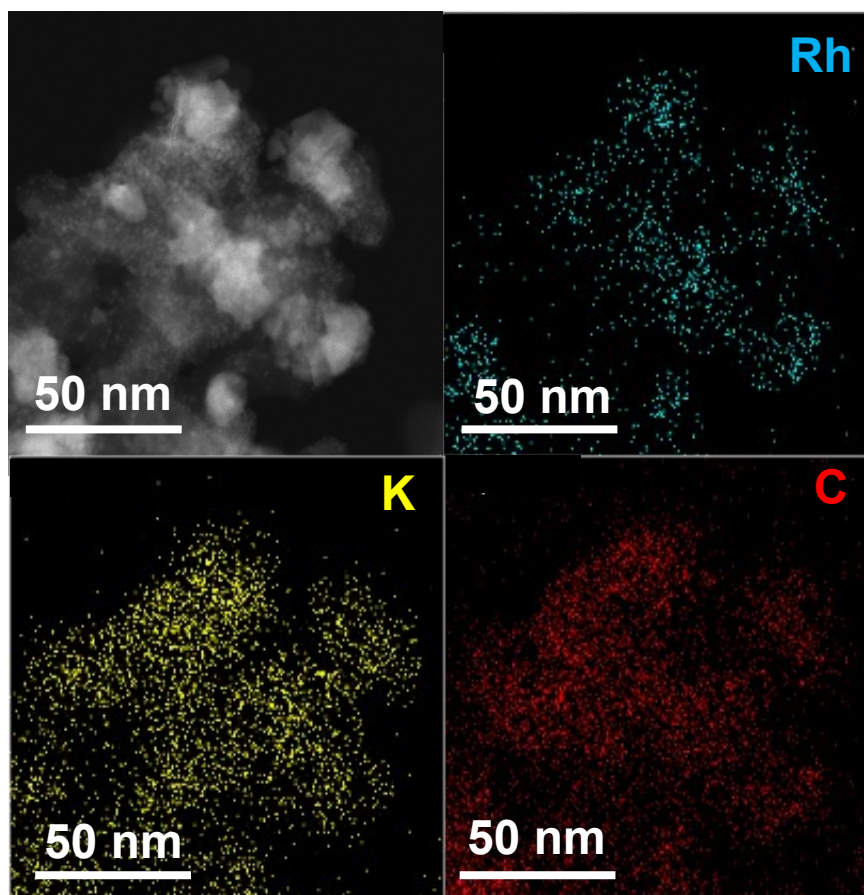Figure S7. TEM image of the spent RhK/AC catalyst.

Figure S8. HAADF-STEM image and the corresponding EDS elemental mapping images of the spent RhK/AC catalyst.
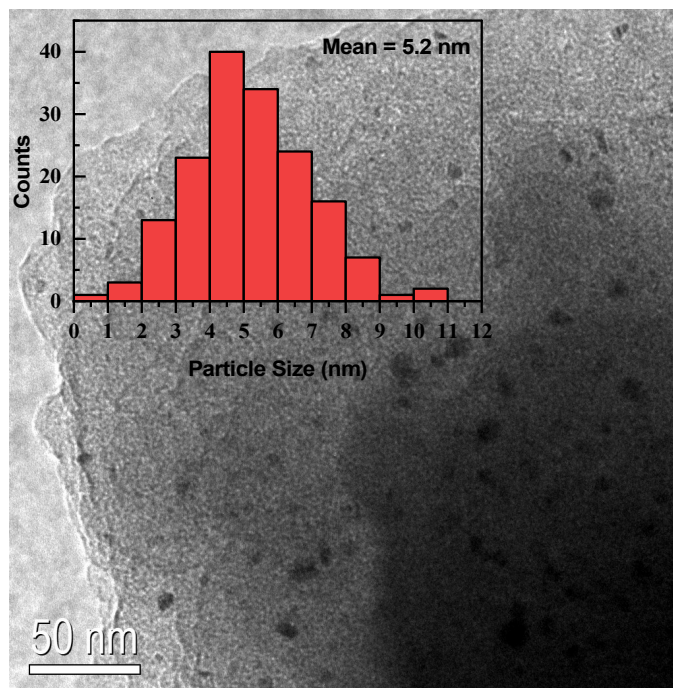

Figure S9. TEM image of the spent Rh/AC catalyst with size distribution of Rh nanoparticles.